SCREEN-PRINTED RIBBON GROWTH ON SUBSTRATE SOLAR CELLS APPROACHING 12% EFFICIENCY

S. Seren[1], G. Hahn[1], A. Gutjahr[2], A. R. Burgers[2], A. Schönecker[2]
[1]University of Konstanz, Faculty of Physics, 78457 Konstanz, Germany
[2]ECN - Solar Energy, P.O. Box 1, 1755 ZG Petten, Netherlands

ABSTRACT

Ribbon Growth on Substrate (RGS) solar cells have been processed at the University of Konstanz using an adapted industrial-type fire-through SiN process. An efficiency of 12.3% has been reached on a 5x5 cm^2 cell. This is the highest efficiency obtained on this very promising and cost-effective material using an industrial-type cell process. An important factor for the increase in efficiency was the reduced oxygen concentration of almost an order of magnitude in the current RGS wafer material compared to former RGS material. Enhanced J_{sc}, V_{oc} and L_{eff} values in the range of 100 µm as well as lifetimes above 4 µs demonstrate the potential of the new low oxygen RGS material. Efficiencies well above 13% should be possible, provided a surface texture is applied and shunting mechanism can be avoided.

INTRODUCTION

A common advantage of all silicon ribbon materials is the high silicon material utilization, which reduces the wafer manufacturing costs (no slicing, no ingot casting). Therefore solar cells processed out of ribbon materials are providing the highest potential in cost reduction per W_p. RGS silicon [1,2] is produced according to a horizontal growth technique in contrast to other silicon ribbon materials produced according to vertical ribbon growth techniques. The main difference between the RGS technique and other ribbon materials is the very high production rate of RGS which allows pulling speeds of v_p ~10 cm/s. The principle of the RGS wafer production technique is shown in Fig. 1. Substrates are pulled underneath the molten silicon inside a casting frame. The wafer crystallizes on the reusable substrate, which absorbs the crystallization heat. Decoupling of crystallization and pulling direction allows the very fast pull speeds in combination with a slow crystallization velocity.

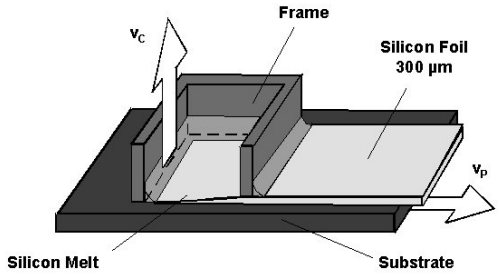

Fig. 1: Principle of the RGS wafer production technique.

Screen-printed RGS solar cells (5x5 cm^2) achieved efficiencies up to 10.5% using RGS wafer material with a high oxygen content of $[O_i] > 10^{18}$ cm^{-3} [3]. These high oxygen concentrations limited solar cell efficiencies due to enhanced recombination at several oxygen related defects such as oxygen precipitates as well as New Donors, which form during wafer production or high temperature solar cell processing steps. The high oxygen content also caused an extremely slow reaction of the RGS material to hydrogen passivation. In order to overcome both limitations, the RGS wafer manufacturing process was improved. This resulted in RGS wafers with lower oxygen contents $[O_i]$ down to $4x10^{17}$ cm^{-3}, which is comparable to standard cast multi-crystalline material. In this paper the main focus is on the characteristics of these low oxygen wafers and their behavior in an industrial-type solar cell process.

CELL PROCESS

RGS wafers are currently produced by a laboratory scale R&D machine at ECN. Due to the substrate size, RGS wafers have dimensions of 8x12 cm^2 and are cut in 5x5 cm^2 wafers by a laser.

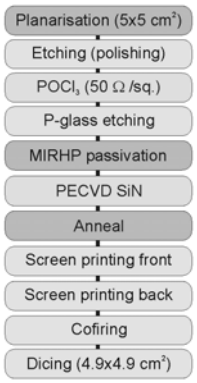

Fig. 2: Applied screen-printing process at UKN. A planarization of the uneven RGS wafer surface is applied as well as an optimized hydrogenation of bulk defects.

Before processing at the University of Konstanz (UKN) the uneven front surface of the wafer is leveled using a wafer-dicing saw in combination with a special planarization tool. After removing the saw damage by acidic polish etching, a 50 Ω/sq. emitter is formed by $POCl_3$ diffusion. A microwave-induced remote hydrogen plasma (MIRHP) passivates bulk defects followed by the deposition of a hydrogen-rich PECVD SiN_x layer, which acts as single layer antireflective coating. Optionally, an annealing step at 600°C can be carried out to release a fraction of the hydrogen originating from the SiN_x layer into the bulk as diffusivity of hydrogen is slowed down in oxygen rich materials. After screen-printing of front and backside metallisation a cofiring step forms the electrical contacts as well as an aluminum back surface field. During the high temperature cofiring step, hydrogen is again released into the bulk. With this combination of hydrogen treatments (hydrogen originating from the

0-7803-8707-4/05/$20.00 ©2005 IEEE.

MIRHP passivation as well as from the SiN_x layer) an optimized passivation of bulk defects is ensured.

CORRELATION OF $[O_i]$ AND J_{sc}

Due to the rapid cooling of the cast RGS wafers after crystallization of the liquid silicon, the formation of oxygen precipitates is inhibited and the oxygen stays preferentially dissolved on interstitial sites in the Si lattice. The concentration of the interstitial oxygen $[O_i]$ in the RGS wafers is determined by FTIR measurements as well as the concentration of the substitutional carbon $[C_s]$.

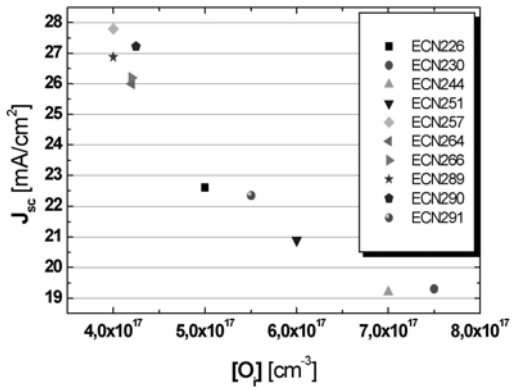

Fig. 3: Dependence of J_{sc} on the interstitial oxygen concentration $[O_i]$ for cells produced from various RGS production runs. Shown are average J_{sc} values of the respective solar cell runs.

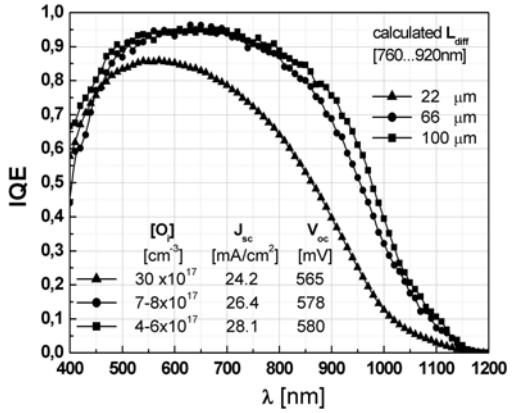

Fig. 4: Increase of the diffusion length with lowered interstitial oxygen concentration $[O_i]$ for 3 representative cells produced from different RGS material.

Fig. 3 shows a clear correlation between lower interstitial oxygen concentrations in the as-grown wafer and a higher J_{sc} of the processed solar cell. Furthermore, a lower oxygen concentration results in larger diffusion lengths as can be seen in Fig. 4 and in a faster hydrogenation [4].

With the lowering of the oxygen content in the RGS wafer material shunt resistances of the processed solar cells seem to be affected. Fits to the dark IV curves revealed sometimes low shunt resistances resulting in poor fill factors for the low oxygen material.

CELL RESULTS

screen printed RGS cell	**V_{oc}** [mV]	**J_{sc}** [mA/cm^2]	**FF** [%]	**η** [%]
high $[O_i]$				
4.9x4.9 cm^2	565	24.2	76.3	10.4
low $[O_i]$				
4.9x4.9 cm^2	580	28.1	75.6	12.3

Table 1: IV data of one of the best screen-printed RGS cells from low $[O_i]$ RGS and high $[O_i]$ RGS (older material) processed at UKN.

The best cell produced from low $[O_i]$ RGS material (run ECN287) achieved a record efficiency of 12.3%. This result was confirmed by a measurement at an ISO 17025 accredited calibration laboratory, namely the European Solar Test Installation (ESTI) of the Joint Research Centre (JRC) of the European Commission.

Compared to solar cells processed from high $[O_i]$ RGS material, J_{sc} as well as V_{oc} could be enhanced resulting in higher efficiencies even though fill factors dropped most probably due to carbon related shunts in low $[O_i]$ material. As soon as these material induced shunts can be avoided, efficiencies above 13% should be reachable. A further enhancement of J_{sc} could already be demonstrated by an acidic texturing of the surface in recent experiments.

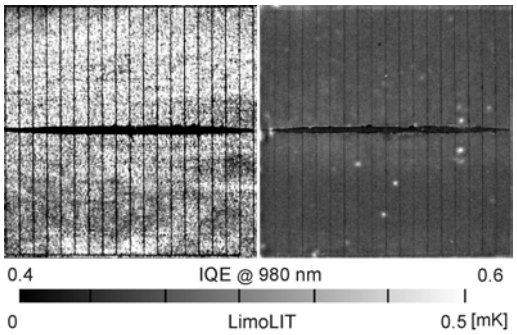

Fig. 5: Left: IQE at 980 nm of the best low $[O_i]$ cell. Right: LimoLIT measurement of the same cell.

The left side of Fig. 5 shows quite homogeneously distributed areas of higher IQE at 980 nm of the best low $[O_i]$ cell. On the right side of Fig. 5 a Light-modulated Lock-In Thermography (LimoLIT [5]) measurement of the same cell is depicted. In contrast to the regions of higher IQE shown in Fig. 7 (left), these regions shown in Fig. 5 are not correlated with regions showing significant heat production. In contrast to expanded shunted regions visible in Fig. 6 only small point like shunts (bright points)

occur partially located under grid fingers indicating rather process induced than material induced shunts. The homogeneity in the IQE of this particular wafer together with the absence of stronger shunted areas results in a quite good fill factor, which enables the achieved efficiency of 12.3%.

SHUNTING IN LOW [O_i] RGS

To investigate the poor shunt resistances sometimes occurring in the low [O_i] RGS wafer material, Voltage-modulated Lock-In Thermography measurements (VomoLIT [5]) were performed on the processed solar cells. The left side of Fig. 6 shows widespread shunted regions (bright areas) under forward bias. The measurement performed on the same cell in reverse bias (Fig. 6, right) showed that nearly all shunts have an ohmic-type character. Only one (marked with a circle) shows a distinct Schottky-type behaviour.

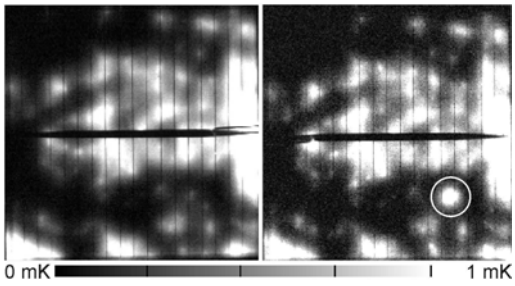

Fig. 6: VomoLIT measurements in forward (+500 mV, left) and reverse (-500 mV, right) bias of a solar cell originating from low [O_i] RGS material (run ECN257). The same widespread shunted regions dropping the fill factor of the solar cell to 55% are visible with an additional Schottky-type shunt in the reverse biased measurement.

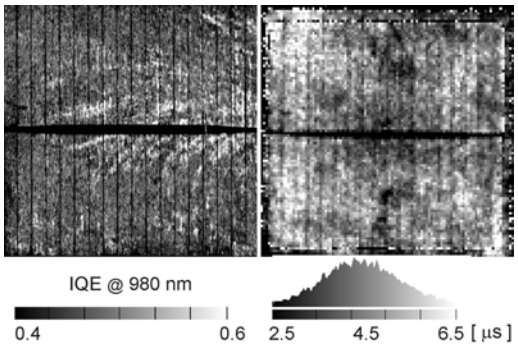

Fig. 7: Left: IQE at 980 nm of the same solar cell as shown in Fig. 6. The widespread shunted regions shown in the thermography mappings are correlated to regions of enhanced IQE. Right: lifetime mapping of the same solar cell after removing of metal contacts, back surface field and emitter. The widespread shunted regions shown in the thermography mappings can be related to regions with lower lifetimes.

Average lifetimes > 4 µs were measured in shuntless regions of low [O_i] RGS. In contrast to that, shunted regions show poor lifetimes (Fig. 7, right) but sometimes an enhanced IQE (Fig. 7, left). Therefore the enhanced IQE in these regions is not correlated to larger diffusion lengths. In these areas shunts are related to a current collecting mechanism, which draws off charge carriers generated next to the shunted regions.

DISCUSSION

Current collection was already observed in high [O_i] RGS material. It was stated that due to oxygen precipitates current collecting inversion channels were formed [6]. As [O_i] is reduced in the current material, it is unlikely that oxygen precipitates are causing the shunts. Due to the carbon supersaturation, a possible explanation of the effect shown in Fig. 7 might be the existence of SiC precipitates, which will be discussed in the following. Although further experiments are needed to clarify the details of the shunting mechanism a number of experimental results are available.

The RGS material contains a high concentration of substitutional carbon in the range of [C_s] = 1.2-1.8x10^{18} cm^{-3}. This supersaturation, possibly supported by the presence of [O_i], will result in the formation of carbon precipitates especially at the bottom and the top of the wafer (Fig. 8). In these wafer regions emitter and back surface field are formed during the following solar cell process steps. Carbon precipitates, respectively SiC formations located in the space charge region of the emitter could then form a conductive path between emitter and base.

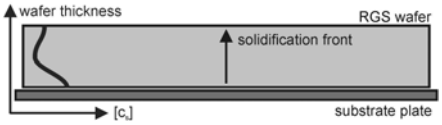

Fig. 8: Distribution of the substitutional carbon concentration [C_s] in a RGS wafer. Local FTIR measurements showed that the carbon concentration is higher at the front and the rear surface of the wafer.

The resulting current flow over such a current path can then produce heat (Fig. 6). It can also be expected that the SiC particles are not distributed homogeneously over the entire wafer due to a preferred precipitation of [C_s] near grain boundaries. Lu et al. [7] measured IR absorption spectra for different [O_i] and after different annealing treatments at varying time and temperatures in RGS wafer material. It was found that low [O_i] is leading to larger carbon precipitates and that the precipitate density was lower in the center of a grain and higher near grain boundaries after annealing at high temperatures. As RGS silicon shows an inhomogeneous grain structure with an average grain diameter in the 0.1-0.3 mm range it would be interesting to examine the correlation between shunt locations and grain size. If a low SiC precipitation density already causes conducting paths throughout the wafer, the observed intra grain depletion of [C_s] in combination

with the precipitation of SiC near grain boundaries should result in higher shunt densities in small grain areas (Fig. 9). If a minimum precipitation density is needed to generate the conducting shunt paths along grain boundaries, larger grain areas are more likely to be shunted.

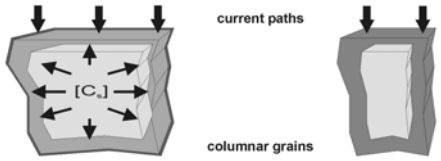

Fig. 9: Columnar grains of different sizes. The carbon is assumed to precipitate preferably at the grain boundaries. The distribution of the current flowing in a large grain might be separated in a current path over the grain itself and the precipitates located at the grain boundary. Considering smaller grains the current flow is assumed to be enabled predominantly by the grain boundary.

In summary, the widespread shunted regions shown in Fig. 6 are assumed to be caused by reticulated carbon precipitates propagating through the entire wafer. SiC related defects typically produce ohmic-type shunts [8] which might explain the predominantly ohmic-type behavior of the shunted regions. Furtheron C precipitates in the form of dendrites were observed [9], which tend to follow grain boundaries.
In order to understand the real mechanism of the shunt paths and the mechanism of its generation in RGS wafers further research is needed.

SUMMARY

Solar cells processed from RGS wafer material with reduced oxygen content using an industrial-type screen-printing firing through SiN process show increased J_{sc} values. Efficiencies up to 12.3% could be reached despite of relatively low fill factors up to 75% on untextured wafers.
Carbon correlated shunted regions in the wafer material itself seem to be responsible for the lower fill factors. These shunted regions in the wafer material itself were visualized by Lock-In Thermography in forward and reverse bias. They show an ohmic-type behavior and are most probably related to carbon precipitates accumulating preferentially at grain boundaries. Due to segregation of dissolved carbon it can be expected that the substitutional carbon concentration [C_s] increases from the bottom to the top of the wafer. Thus SiC precipitates are likely to occur in the emitter region of the solar cell causing alternative ohmic current paths and current dissipation through the space charge region.

OUTLOOK

Enhanced J_{sc} and V_{oc} values demonstrate already the potential of the low [O_i] RGS material to reach efficiencies well above 13%, provided a surface texture is applied and shunting mechanisms can be avoided. Different surface texturing methods are currently investigated to increase J_{sc}.

In order to reduce shunting in low [O_i] RGS wafer material, the carbon concentration has to be reduced. This should lead to better fill factors and therefore to higher efficiencies.

Due to a faster hydrogenation in low [O_i] RGS material the duration and the temperature of an additional microwave induced remote hydrogen plasma (MIRHP) bulk passivation could already be reduced significantly. The intention is to omit the MIRHP bulk passivation in general, to end up with a totally industrial compatible solar cell process.

ACKNOWLEDGEMENTS

Part of this work was funded by the EC in the RGSells project (ENK6-CT-2001-00574). The RGS wafer manufacturing process development is carried out in the RGSolar project supported by the EET programme under EETK 03023.

LITERATURE

[1] H. Lange et al. "Ribbon Growth on Substrate (RGS) - A new approach to high speed growth of silicon ribbons for photovoltaics", *J. Cryst. Growth*, 104 (1990) 108

[2] W. Koch et al. "Preparation, characterisation and cell processing of Bayer RGS silicon foils (Ribbon Growth on Substrate)", *Proc. 2nd WC PVSEC*, Vienna 1998, 1254

[3] G. Hahn et al. "Over 10% efficient screen printed RGS solar cells", *Proc. 3rd WCPEC PVSC*, Osaka 2003

[4] G. Hahn et al. "Hydrogenation of multicrystalline Silicon - The Story continues", *Proc. 19th EC PVSEC*, Paris 2004

[5] M. Kaes et al. "LimoLIT – A novel Thermographic Characterisation Method for p/n Structures and Solar Cells", *Proc. 19th EC PVSEC*, Paris 2004

[6] G. Hahn et al. "Current collecting channels in RGS silicon solar cells - are they useful?", *Sol. Energy Mat.* 72 (2002) 453-464

[7] J. Lu et al. "Infrared absorption of SiC precipitates in crystalline silicon: experimental data and theoretical interpretation", submitted to *Appl. Phys. Lett.*, 2004

[8] H. Gottschalk "Precipitates in Ribbon Grown Solar Silicon", *phys. stat. sol.* (b), p. 353 (2000)

[9] M. Hejjo Al Rifai et al. "Investigation of Material-Induced-Shunts in Block-Cast Multicrystalline Silicon Solar Cells Caused by SiC Precipitate Filaments", *Proc. 19th EC PVSEC*, Paris 2004